The Journal of Chemical Physics

Reference dependence of the two-determinant coupled-cluster method for triplet and open-shell singlet states of biradical molecules

Cite as: J. Chem. Phys. **148**, 164102 (2018); https://doi.org/10.1063/1.5025170
Submitted: 07 February 2018 . Accepted: 09 April 2018 . Published Online: 24 April 2018

Jesse J. Lutz, Marcel Nooijen, Ajith Perera, and Rodney J. Bartlett

Reference dependence of the two-determinant coupled-cluster method for triplet and open-shell singlet states of biradical molecules

Jesse J. Lutz,[1,2,a)] Marcel Nooijen,[3] Ajith Perera,[2] and Rodney J. Bartlett[2]
[1]*Air Force Institute of Technology, Wright-Patterson Air Force Base, Ohio 45433, USA*
[2]*Quantum Theory Project, University of Florida, Gainesville, Florida 32611, USA*
[3]*Department of Chemistry, University of Waterloo, Waterloo, Ontario N2L 3G1, Canada*

(Received 7 February 2018; accepted 9 April 2018; published online 24 April 2018)

We study the performance of the two-determinant (TD) coupled-cluster (CC) method which, unlike conventional ground-state single-reference (SR) CC methods, can, in principle, provide a naturally spin-adapted treatment of the lowest-lying open-shell singlet (OSS) and triplet electronic states. Various choices for the TD-CC reference orbitals are considered, including those generated by the multi-configurational self-consistent field method. Comparisons are made with the results of high-level SR-CC, equation-of-motion (EOM) CC, and multi-reference EOM calculations performed on a large test set of over 100 molecules with low-lying OSS states. It is shown that in cases where the EOMCC reference function is poorly described, TD-CC can provide a significantly better quantitative description of OSS total energies and OSS-triplet splittings. *Published by AIP Publishing.*
https://doi.org/10.1063/1.5025170

I. INTRODUCTION

Single-reference (SR) methods based on the exponential wavefunction ansatz of coupled-cluster (CC) theory are the most successful electronic structure methods for the calculation of energies and properties of atomic and molecular systems in their ground and excited states.[1–3] Notable strengths of CC theory when compared with other *ab initio* methods, and first-principle but not *ab initio* ones like Kohn-Sham (KS) density functional theory (DFT), are that it is size-extensive, it provides a good balance of static and dynamical correlation, and it converges systematically to the full configuration interaction (CI) limit. The most widely used CC approximations are CC with singles and doubles (CCSD)[4] and its extension including a perturbative correction for triple excitations known as CCSD(T).[5–7] In the past, CC methods were severely limited by their well-known steep polynomial scaling ($\mathcal{N}^6$–$\mathcal{N}^7$) of the serial computing cycles with the number of correlated orbitals ($\mathcal{N}$). Fortunately, this polynomial scaling, which makes performing calculations prohibitively expensive for most extended systems, is rapidly being overcome through massively parallel computing algorithms[8,9] plus orbital localization schemes.[10–16] These advances, which make CC-quality energies and properties obtainable at near-DFT cost,[17] provide a new stimulus for the further development of CC methods that are likely to find renewed interest within a more computationally tractable framework.

A major obstacle to the direct application of the SR-CC formalism to excited states is its inability to treat open-shell states such as open-shell singlet states (OSSs), the most common type of excited state. Though there is great flexibility in the starting point for SR-CC, in practice the ansatz requires that the zeroth-order initial guess of some single determinant be a "sufficiently accurate" starting approximation to the overall wavefunction expansion. The variety in use—restricted Hartree-Fock (RHF), unrestricted Hartree-Fock (UHF), restricted open-shell Hartree-Fock (ROHF), Brueckner (B), the first natural determinant, Kohn-Sham, quasi-restricted Hartree-Fock (QRHF), and CC orbital optimized—provide important flexibility in this choice. However, open-shell states require more than one determinant in the zeroth-order to form a spin-adapted configuration state function (CSF). Thus, the pursuit of open-shell states within CC theory normally leads to either (1) multi-reference (MR) CC methods of either the Fock space or Hilbert space (HS) variety[18] or (2) excited-state SR-CC methods like the equation-of-motion (EOM) CC where excitation (or de-excitation) operators are applied to a related SR-CC function to form the target low-spin state.[19] Due to the complications which arise in the formulation and application of MR-CC methods,[18] the EOMCC approaches[20–22] have become widely adopted for routine use.

EOMCC and its linear-response CC counterparts[23–28] build the desired excited-state information using as a reference the SR-CC ground state wavefunction. The EOMCCSD method can be extended to achieve greater accuracy, in analogy to the ground-state case, by adding triple excitations perturbatively, as in the EOMCCSD(T) method,[29–32] or iteratively, from EOMCCSDT-*n* to the full EOMCCSDT. The results of the EOMCCSD method depend on the quality of the correlated ground state reference that, ideally, should be such that the excited-state function is accessible by largely single excitations out of the reference. Although orbital choice

a)Electronic mail: jesse.lutz.ctr@afit.edu

in SR-CCSD and beyond has very little effect on the ground state, it might affect the quality of the EOMCCSD target states. For example, employing KS orbitals has been shown to be a viable alternative for systems with nearly degenerate states.[33] Additionally, other orbital choices, such as those taken from Brueckner theory,[34,35] may also be advantageous in certain situations.

If instead high-spin states are of interest, standard SR-CC theory can be employed in a straightforward manner by using as a reference the UHF or ROHF wavefunctions,[7,36,37] or any of the others mentioned above in their high-spin variants. The UHF reference leads to a lowering of the total energy as compared with the restricted variants and it introduces important spin-polarization effects on the spin density, but a price is paid for allowing α-spin electrons to occupy different spatial orbitals than the β-spin electrons. First, the resulting reference determinant is not an eigenfunction of spin, $\langle \hat{S}^2 \rangle$, and second, having to treat different orbitals for different spins usually requires ∼3 times the computer time as in the RHF reference case. The situation is not much better for the spin-symmetry-preserving ROHF-based formalism. The reference determinant is an eigenfunction of spin but the CC wavefunction is not, just as in the UHF-CC case, so the multiplicity, $2S+1 \approx \sqrt{1+4\langle S^2 \rangle}$, should be monitored.[38] One exception is the EOMCCSD approach of Szalay and Gauss,[39] which creates EOMCC states based upon a ROHF ground-state CC solution that are proper spin-eigenfunctions. However, most methods based upon ROHF wavefunctions encounter formidable and problematic symmetry-breaking issues which cause additional complications.[40]

An alternative approach to EOMCC for directly obtaining the open-shell singlet and its $M_s = 0$ triplet partner is provided by the two-determinant (TD) CC method, the subject of this paper. The TD-CC method is a special case of the state-universal (SU) HS MR-CC method initially formulated by Kucharski and Bartlett[41] but is specifically geared toward describing OSS states.

TD-CC has several attractions:

(1) It is the simplest-possible, justified starting-point for an open-shell singlet. (SR-CC with UHF low-spin states provides a 50-50 mixture of the singlet and triplet.)
(2) Unlike EOMCC which uses a linear operator, $\widehat{\mathbf{R}}_k$, to describe the target state, it uses an exponential form. It is thus fully linked and size-extensive.
(3) It introduces selected triple excitations efficiently as single and double excitations from the second determinant, rather than having to add R_3 into EOMCC.
(4) It provides the $M_s = 0$ singlet and triplet pairs simultaneously.
(5) It is highly interpretive as it identifies a particular excitation from i → a (occupied orbital i to unoccupied orbital a) as the zeroth-order function for the TD-CC wavefunction.
(6) In principle, TD-CC can provide spin-pure open-shell states, but the current ACESII[42] implementation is a spin-orbital one.
(7) The TD-CCSD approximation has the same (N^6) computational scaling as conventional SR-CCSD.
(8) Low-spin doublet states and others that are fixed by spin-symmetry could be similarly described as in the TD-CCSD theory presented below.

The TD-CCSD method has been applied previously to methylene,[43] cyclobutadiene,[44] water,[45] and ketene and diazomethane.[46] Analytic gradients were also implemented, enabling a thorough analysis of the energies, geometries, and frequencies of *trans*-butadiene and ozone.[47] Efficient and general spin-orbital implementations of TD-CCSD are currently available in the ACESII, CFour,[48] and MOLCAS[49] software packages. A related orthogonally spin-adapted formulation of TD-CCSD was derived, implemented, and applied by Piecuch *et al.*,[50–56] but those codes were not distributed publicly.

In this work, we return to examine the accuracy and formal properties of TD-CCSD as it is currently implemented in ACESII. Of particular interest is the performance of TD-CCSD relative to the ROHF/SR-CCSD results for lowest-lying triplet states (T_0) and relative to the RHF/EOMCCSD results for both T_0 states and their companion OSS states. In the following, we will abbreviate OSS states as S_1, while noting that in certain cases, a multi-reference closed-shell singlet may lie between the closed-shell ground-state singlet (S_0) and the S_1 state (see, e.g., Ref. 57). The energy gap between them, the singlet-triplet ($S_1 - T_0$) splitting, also warrants attention. The quality of the results will be investigated in terms of the accuracy of absolute and relative energetics.

For these tests, we have chosen a variety of computationally tractable systems commonly known to have ground-states with a significant biradical character (see also, Ref. 58). For such states SR-CCSD will usually provide a poor ground-state description, and consequently the RHF/EOMCCSD has difficulty adequately recovering some correlation effects. It is thus an interesting question whether direct application of the CC ansatz to the relevant excited state can produce a better description than RHF/EOMCCSD. Hence, this paper provides TD-CCSD energies for a large set of demanding molecules.

The purpose of this study is to benchmark the TD-CCSD approach and the choice of reference energy values is delicate. The TD-CCSD approach does not include triple excitations and for this reason the most meaningful comparison would be against a multi-reference approach that works with similar small active spaces as TD-CCSD, which includes singles and doubles only. Our method of choice is the MREOM approach which has shown to give excellent results for atomic excitation spectra,[59] excitation spectra of organic molecules,[60] and a limited set of transition metal compounds.[61]

In MREOM, a sequence of similarity transformations of the Hamiltonian is performed and the final state energies are obtained by a compact diagonalization over the complete active space (CAS) plus 1-hole + 1-particle excitations. The similarity transformations account in a size-extensive way for all other excitations, and many electronic states can be obtained in a balanced way based on a single state-averaged (SA) CAS to define the orbitals and a single set of transformation amplitudes.

The structure of this paper is as follows. Section II describes the theory underlying the TD-CCSD method and a

formal justification is given that builds an expectation for good performance when employing particular reference orbitals. Section III describes procedural details and approximations used in this work, including the choice of basis set and electronic structure packages employed. Section IV outlines the systems studied, compares TD-CCSD results generated using a variety of reference orbitals, and provides a comparative evaluation of the performance of TD-CCSD for producing triplet and OSS energies. Section V recapitulates our conclusions.

II. THEORY

Here we briefly summarize and discuss the derivation and implementation of the equations for the TD-CC energy and amplitudes. This is done primarily to point out the key approximations made during the procedure. The full derivation of the energy and analytic derivative equations, including full expressions for the renormalization terms for CASs and incomplete active spaces (IAS) can be found in Ref. 47. We conform to that notation in the following.

The formulation of the TD-CC equations begins with the construction of an appropriate reference space, P, which for the special case of TD-CC is restricted to be the two determinants that define the OSS and associated triplet wavefunction,

$$ {}^{A}\Phi = \bar{n}^{\dagger} m^{\dagger} \prod_{i} i^{\dagger} |vac\rangle, \; {}^{B}\Phi = n^{\dagger} \bar{m}^{\dagger} \prod_{i} i^{\dagger} |vac\rangle. $$

Here lower-case letters with daggers mean creation operators, with $i, j, \ldots$ designating occupied spin orbitals and $a, b, \ldots$ designating virtual spin orbitals, m and n represent open-shell spin-orbitals (unbarred with α spin and barred with β spin), and $|vac\rangle$ is the true vacuum.

The Bloch equation used in MR-CC[62] is

$$ H\Omega = \Omega H \Omega = \Omega H^{\text{eff}}, $$

where Ω is the waveoperator, which transforms a model function defined in the model space spanned by P to the exact wavefunction. $\mathrm{H}^{\text{eff}} = PH\Omega P$, which in this case will be a 2×2 matrix.

The two "model" functions are thus

$$ {}^{S}\Psi_0 = \frac{1}{\sqrt{2}}({}^{A}\Phi + {}^{B}\Phi), \; {}^{T}\Psi_0 = \frac{1}{\sqrt{2}}({}^{A}\Phi - {}^{B}\Phi) $$

of singlet and triplet multiplicity, respectively. Because they are of different spin symmetries, the H^{eff} will block into two solutions, an OSS part, $\langle {}^{S}\Psi_0 | H^{\text{eff}} | {}^{S}\Psi_0 \rangle$, and a triplet part, $\langle {}^{T}\Psi_0 | H^{\text{eff}} | {}^{T}\Psi_0 \rangle$.

To form the MR-CC singlet (triplet) state, the ${}^{S}\Psi_0$ (${}^{T}\Psi_0$) reference function is operated on using the conventional Jeziorski-Monkhorst (JM) waveoperator[63] that here takes the form

$$ \hat{\Omega} = [e^{T_A} | {}^{A}\Phi \rangle \langle {}^{A}\Phi |] + [e^{T_B} | {}^{B}\Phi \rangle \langle {}^{B}\Phi |], $$

with $T_A (T_B)$ being the usual cluster operator of CC theory defined with respect to the Fermi vacuum ${}^{A}\Phi ({}^{B}\Phi)$. At this point, a term is explicitly removed from the equations, which corresponds to the active-active double excitation creating ${}^{B}\Phi$ from ${}^{A}\Phi$ and vice-versa, because that would be a redundant (internal) determinant.

Solutions for these equations are obtained in the usual way by choosing a level of truncation for the cluster operators. Here we choose to truncate the cluster operator to include only single and double excitations. Thus after enforcing the projectors in the waveoperator, the expressions for the OSS state correlation energy is

$$ \begin{aligned} \Delta E &= \langle {}^{A}\Phi | H_N e^{T_A} | {}^{A}\Phi \rangle + \langle {}^{A}\Phi | H_N e^{T_B} | {}^{B}\Phi \rangle \\ &\equiv \Delta E_A + W, \end{aligned} $$

while the corresponding triplet correlation energy is $\Delta E = \Delta E_A - W$. Projections onto the subspaces of singly and doubly excited determinants produce equations for the determination of the t_1 and t_2 amplitudes, respectively, and they are given as

$$ \begin{aligned} \mathcal{Q}_i^a &= \langle {}^{A}\Phi_i^a | H_N e^{T_A} | {}^{A}\Phi \rangle_C - \left(\langle {}^{A}\Phi_i^a | e^{T_B} | {}^{B}\Phi \rangle \langle {}^{B}\Phi | H_N e^{T_A} | {}^{A}\Phi \rangle \right)_C \\ &\equiv \langle {}^{A}\Phi_i^a | H_N e^{T_A} | {}^{A}\Phi \rangle_C + M_i^a W = 0 \end{aligned} $$

and

$$ \begin{aligned} \mathcal{Q}_{ij}^{ab} &= \langle {}^{A}\Phi_{ij}^{ab} | H_N e^{T_A} | {}^{A}\Phi \rangle_C - \left(\langle {}^{A}\Phi_{ij}^{ab} | e^{T_B} | {}^{B}\Phi \rangle \langle {}^{B}\Phi | H_N e^{T_A} | {}^{A}\Phi \rangle \right)_C - P(ij, ab) \Big[\langle {}^{A}\Phi_i^a | e^{T_A} | {}^{A}\Phi \rangle \\ &\quad \times \left(\langle {}^{A}\Phi_j^b | e^{T_B} | {}^{B}\Phi \rangle \langle {}^{B}\Phi | H_N e^{T_A} | {}^{A}\Phi \rangle \right)_C - \hat{R}(ia) \langle {}^{B}\Phi_i^a | e^{T_B} | {}^{B}\Phi \rangle \left(\langle {}^{A}\Phi_j^b | e^{T_B} | {}^{B}\Phi \rangle \langle {}^{B}\Phi | H_N e^{T_A} | {}^{A}\Phi \rangle \right)_C \Big] \\ &\equiv \langle {}^{A}\Phi_{ij}^{ab} | H_N e^{T_A} | {}^{A}\Phi \rangle_C + M_{ij}^{ab} W = 0, \end{aligned} $$

where the subscript C means that only connected terms are included, $\hat{R}(ia) = (1 - \delta_{in_\alpha})(1 - \delta_{im_\beta})(1 - \delta_{am_\alpha})(1 - \delta_{an_\beta})$, i.e., the effect of operator $\hat{R}$ is that in all preceding terms only inactive (double occupied and virtual) labels are included. Explicit expressions for calculation of the renormalization terms, M_i^a and M_{ij}^{ab}, can be found in Ref. 47. The Hamiltonian is normal ordered with respect to determinant ${}^{A}\Phi$,

$$ H = \langle {}^{A}\Phi | H | {}^{A}\Phi \rangle + \sum_{pq} f_{pq} \{ p^{\dagger} q \} + \frac{1}{4} \sum_{pqrs} \langle pq || rs \rangle \{ p^{\dagger} q^{\dagger} sr \}, $$

where $\{\}$ means normal ordering, f_{pq} is the matrix element of the usual Fock operator, and $\langle pq || rs \rangle$'s are antisymmetrized two-electron integrals.

At this point, a second set of equations can also be derived using ${}^{B}\Phi$ in the projections to obtain as many equations as

amplitudes in T_B as in T_A, but this is not necessary. As originally suggested in Ref. 46, since ${}^A\Phi$ and ${}^B\Phi$ are related by a single spin flip, so too should be the T_A and T_B operators. This relation leads to implementing the method in a fashion as close as possible to the SR-CC theory, basing it upon only one determinant, and effects reduction in the computation time by a factor of two in the current ACESII implementation. It can be verified computationally that identical results are obtained whether the user initially forms ${}^A\Phi$ or ${}^B\Phi$ as the effective "single" reference.

Methods based on the HS-MRCC framework fall into various categories based on symmetry classifications of the determinants included in the model space. Consequently, the TD-CC approach can be one of two variants. If the active TD-CC orbitals are chosen to be of different spatial symmetry (ab-type), then all possible excitations (two) of a given symmetry involving the active orbitals are included in the model space, making it a CAS. On the other hand, if the active TD-CC orbitals are chosen to be of the same spatial symmetry (aa-type), only two of the four CAS determinants are included, making it an IAS variant. The latter was formulated by Meissner *et al.*,[64] where intermediate normalization was relaxed and certain terms made zero to guarantee size-extensivity.

The SU-HS-MRCC method as originally formulated[41] and used[41,44,64,65] always employed a CAS model space and consequently the JM waveoperator Ω always produced excited configurations outside the reference space.[63] As addressed by Meissner *et al.* above, and later shown by Li and Paldus, the exclusion of internal excitations from the cluster operators is not valid for incomplete model spaces.[66] The exclusion of internal excitations from T_A in an IAS method is equivalent to their exclusion from Ω, which can cause an incidental introduction of disconnected-cluster terms that otherwise would normally be canceled by connected-cluster terms in the CAS analog. Disconnected terms could cause other formal aspects of the theory to be disrupted as well. A similar omission is chosen in the λ equations for the analytic derivatives. Here, we use the Meissner IAS formulation. Li and Paldus have also developed a generalized model space SU-MRCC method to address such deficiencies.[40,66–74]

III. COMPUTATIONAL DETAILS

For the computation of the TD-CCSD OSS wavefunction, a zeroth-order CSF is constructed using a procedure involving QRHF determinants (meaning determinants where the orbitals are chosen non-variationally) that was demonstrated to be adequate in previous studies.[43–47] Conventionally the QRHF reference orbitals have been generated by computing the RHF determinant for a related S_0 state, followed by promotion of an electron from an alpha occupied to an alpha virtual, with the direct product of the symmetries of the orbital pair having the desired spatial symmetry of the target state. For all calculations performed in this work, the appropriate transition corresponds to the energetically highest-lying occupied molecular orbital (HOMO) and lowest-lying unoccupied molecular orbitals (LUMO) of the appropriate symmetry, though it should be noted that the QRHF/TD-CC approach is broadly applicable to non-HOMO/non-LUMO transitions as well. In general, TD-CCSD can target and converge upon a number of excited states. However, here the QRHF procedure uses a predetermined orbital occupancy (singly occupied HOMO and LUMO), so the intended excited state is uniquely described by simply specifying reference orbitals together with the method (e.g., RHF/TD-CCSD). This short-hand notation is convenient when comparing different CC methods that use the same set of reference orbitals (e.g., RHF/TD-CCSD and RHF/SR-CCSD).

Several methods are tested for the generation of non-HF reference orbitals. The first is KS-DFT applied to the S_0 state with orbitals obtained using the B3LYP functional. Unlike the RHF method, the KS-DFT approach uses the same potential for the generation of the occupied and the virtual orbitals. Since the TD-CC active space always involves both occupied and virtual orbitals, it is feasible that improved energetics could result from an improved description of the active orbitals. Another method is a simple yet physically motivated unitary transformation of the canonical RHF orbitals, replacing them by a set determined by applying an averaged $N-1$ potential ($\overline{V}^{N-1}$),[75] which is also a kind of generalized Fermi-Amaldi factor.[76] It is well-known that SR-CC is invariant to similarity transformations applied to occupied-occupied and virtual-virtual orbitals. By contrast, application of the $\overline{V}^{N-1}$ potential can have an effect on the TD-CC energetics because within the QRHF procedure, it causes a mixing of one of the occupied orbitals with the virtual space.

To address the question of using multi-configurational (MC) self-consistent field (SCF) reference orbitals, we also generate natural orbitals of the CASSCF method with two electrons in two orbitals CAS(2,2). Natural orbitals are produced from (1) the OSS CSF,[77] (2) the triplet ($M_s = 0$) CSF, which in the field-free case is energetically equivalent to the ROHF ($M_s = \pm 1$) determinant,[78] and (3) the SA-CAS, formed by mixing equally the lowest-lying triplet and OSS two-determinant CSFs.[79] For clarity, here we refer to (1) as TD-SCF, (2) as ROHF, and (3) as SA-MCSCF(2,2). Because this study is primarily interested in $S_1 - T_0$ gaps, we focus on results found using the SA-MCSCF(2,2) reference orbitals since it contains no bias toward either of the two states of interest. For systems with more orbital degeneracy, specification of larger SA-MCSCF active spaces can improve the description of severely multi-reference triplet and OSS configurations.

The DZP basis set of Dunning was used throughout,[80,81] with the hydrogen *p* exponent set to 0.7, the carbon *d* exponent set to 0.654, the fluorine *d* exponent set to 1.58, and the silicon *d* exponent set to 0.28. All correlated calculations were performed with core orbitals frozen. The SR-CC, EOMCC, and TD-CC calculations were performed using ACESII on the University of Florida HiPerGator cluster or ACESIII on the AFRL DSRC SGI Ice X Thunder. In the MREOM calculation, the orbitals are obtained from the SA-MCSCF calculation including the S_1 and T_0 states. The amplitudes included in the transformation step of MREOM include T, S, and U, such that the final diagonalization in MREOM is over CAS + 1-hole + 1-particle excitations. The calculations are performed using the MRCC extension to ACESII developed by the Nooijen group in Waterloo.

IV. RESULTS AND DISCUSSION

In the following, we examine the results of computations performed on a large set of biradical systems taken from Ref. 82. The systems are sketched in Fig. 1 and included among them are several functionalized variants of the following molecule classes: (a) carbenes, (b) silylenes, (c) cyclobutane-1,3-diyls, (d) cyclopentane-1,3-diyls, (e) *ortho*-xylylenes, (f) *meta*-xylylenes, and (g) *para*-xylylenes. The cyclobutanediyls and cyclopentanediyls are abbreviated here as cyclo_4s and cyclo_5s and the xylylene prefixes are abbreviated. This set of systems serves to vary both the number of correlated electrons and the symmetry of the states. Additionally, the configurational isomers of xylylene give insight into the effect of independently varying the level of the non-dynamical correlation. The electronic structure of *m*-xylylene has significant static correlation, as discussed in detail in Refs. 83 and 84. There it is suggested that, unlike for *o*-xylylene and *p*-xylylene, a CAS(2,2) calculation alone is inadequate for the determination of the $S_1 - T_0$ splitting of *m*-xylylene, and they advocate that active spaces as large as (8,8) must be used instead.

As noted in Ref. 82, the four monochlorinated cyclopentanediyl systems were optimized to poor geometries at the UB3LYP/6-31G* level, producing structures with C–Cl bonds that were extended so far (2.4 Å) as to be effectively broken. For this reason, we have re-optimized these four structures using MBPT(2)/6-31G* and obtained R_{C-Cl} values which are shorter by at least 0.6 Å for each molecule. Testing the performance of TD-CCSD along single-bond-breaking potential wells is outside the scope of the present work, but we intend to further address this topic in a subsequent study. In the following, we will use these newly optimized geometries for these four species in our analyses.

A. Consequences of employing non-standard orbitals or the Brueckner variant

In Sec. II, it was mentioned that, unlike SR-CCSD, where the Thouless condition usually guarantees orbital invariance even when mixing occupied and virtual orbitals, employing alternate reference orbitals in the TD-CCSD method might provide an opportunity for improvement. With the objective of obtaining the lowest possible energies within the TD-CCSD scheme, we tested several alternatives for the generation of the reference orbitals. In addition, we tested the effect of Brueckner orbital-optimization. Forcing t_1 amplitudes to become vanishingly small in the B/CC procedure provides another useful check for our study of TD-CCSD since many t_1 amplitude-dependent terms are effectively eliminated from the equations for the energy, amplitudes, and gradients.

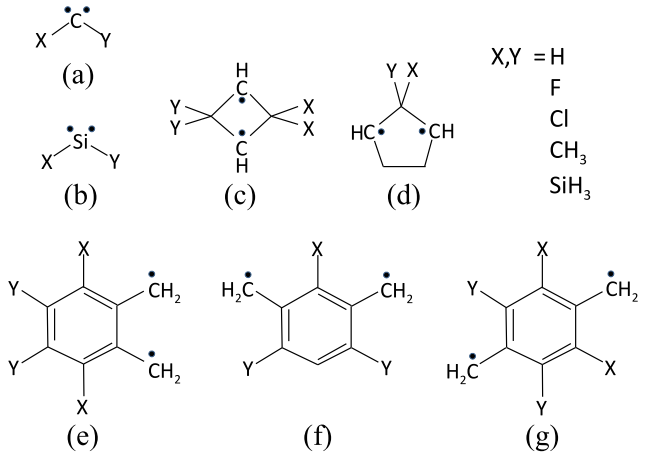

FIG. 1. The full set of molecules (a)–(g) for which singlet-triplet splittings were computed.

Table I collects raw errors and mean unsigned errors (MUE) in the T_0 energy as produced by several coupled-cluster approaches, with benchmark values produced using the ROHF/SR-CCSD(T) method. The first 15 rows provide results for the individual carbenes, while the lower rows provide MUEs including several subsets and the full set of biradicals sketched in Fig. 1. Here it is possible to examine errors side-by-side corresponding to both the aa-type and ab-type transitions, which represent fundamentally different model spaces in the SU-HS-MRCC theory. We note that, as expected, there is no apparent bias in the TD-CCSD errors toward systems with the ab-type classification, reaffirming that the method satisfies the Meissner IAS formulation.

To determine which TD-CC variants are worthwhile for compiling the full set, we first computed smaller subgroups of the biradical systems, starting with the carbenes and silylenes [(a)–(b)]. For this set, the ROHF/SR-CCSD, UHF/SR-CCSD, ROHF/B/SR-CCSD, RHF/EOMCCSD, and RHF/EOMCCSD(T) methods all give MUEs within ∼15% of the lowest MUE, 0.229 eV, produced by ROHF/SR-CCSD. Meanwhile the TD-CCSD method performed similarly well using reference orbitals from the RHF, RHF($\overline{V}^{N-1}$), ROHF, TD-SCF, and SA-MCSCF theories, with the best value, 0.182 eV, given by ROHF/TD-CCSD. The KS/TD-CCSD approach returned a very large MUE, and as such we did not continue compiling those values for the remaining systems. Considering next the first four system classes [(a)–(d)], very similar MUEs were returned for each of the RHF-based TD-CCSD approaches, including RHF/TD-CCSD, RHF/B/TD-CCSD, and RHF($\overline{V}^{N-1}$)/TD-CCSD. The additional expense of the RHF/B/TD-CCSD approach seemed unwarranted, so it was not considered for the full set. For this larger (a)–(d) subgroup, ROHF/TD-CCSD again performed best, giving an MUE 4.2% lower than ROHF/SR-CCSD.

When the full set of biradical systems [(a)–(g)] was analyzed, MUEs of 1.052, 1.165, and 1.195 eV were returned by the ROHF/SR-CCSD, RHF/EOMCCSD, and RHF/TD-CCSD methods, respectively. For the TD-CCSD method, it was found that switching from conventional RHF orbitals to optimized ROHF orbitals resulted in an improvement of over 20%, with ROHF/TD-CCSD providing the best overall MUE of 0.954. The SA-MCSCF(2,2)/TD-CCSD approach, which is the focus of the current study, returned 1.098 eV, which is still lower than the RHF/EOMCCSD MUE by ∼5.0%. Further comparisons of the quality of these methods are made in Subsections IV B–IV D.

The significant improvement in T_0 energies found when moving from RHF/TD-CCSD to ROHF/TD-CCSD suggests that optimization of the reference orbitals in the TD-CCSD

TABLE I. Errors for the lowest-lying triplet total energies as computed using a variety of methods. Where specific systems are not specified, a mean unsigned error (MUE) is given for a group of systems, which are designated using the same labeling convention as Fig. 1. All errors are taken with respect to ROHF/SR-CCSD(T) values, in eV.

		Method/reference												
System	Transition Symmetry	SR-CCSD ROHF	SR-CCSD UHF	B/SR-CCSD ROHF	TD-CCSD RHF	TD-CCSD RHF($\overline{V}^{N-1}$)	TD-CCSD KS	B/TD-CCSD RHF	TD-CCSD ROHF	TD-CCSD TD-SCF	TD-CCSD SA-MCSCF	EOMCCSD RHF	EOMCCSD(T) RHF	MREOM CAS(2,2)
CH_2	ab	0.049	0.047	0.049	0.060	0.045	0.196	0.025	0.040	0.052	0.047	0.053	0.070	0.050
CHF	ab	0.165	0.163	0.091	0.167	0.161	0.477	0.164	0.116	0.157	0.141	0.182	0.204	0.044
CHCl	ab	0.179	0.176	0.196	0.198	0.200	1.127	0.184	0.129	0.164	0.149	0.188	0.205	0.096
$CHCH_3$	aa	0.171	0.168	0.176	0.184	0.175	0.475	0.166	0.147	0.166	0.158	0.182	0.196	0.131
$CHSiH_3$	aa	0.137	0.133	0.141	0.158	0.155	1.157	0.118	0.125	0.136	0.132	0.135	0.140	0.125
CF_2	ab	0.277	0.275	0.326	0.256	0.259	0.715	0.263	0.181	0.259	0.227	0.307	0.342	0.170
CFCl	ab	0.294	0.291	0.331	0.297	0.301	1.390	0.286	0.209	0.274	0.248	0.323	0.342	0.166
$CFCH_3$	aa	0.285	0.284	0.318	0.286	0.280	0.745	0.277	0.223	0.273	0.253	0.311	0.328	0.189
$CFSiH_3$	aa	0.262	0.260	0.298	0.280	0.274	1.469	0.293	0.213	0.248	0.235	0.283	0.295	0.188
CCl_2	ab	0.311	0.307	0.334	0.327	0.332	2.055	0.300	0.235	0.288	0.267	0.330	0.347	0.158
$CClCH_3$	aa	0.302	0.299	0.318	0.317	0.317	1.402	0.281	0.244	0.284	0.268	0.320	0.334	0.187
$CClSiH_3$	aa	0.278	0.274	0.297	0.303	0.300	2.108	0.280	0.232	0.232	0.249	0.294	0.306	0.174
$C(CH_3)_2$	aa	0.297	0.295	0.307	0.310	0.302	0.756	0.303	0.262	0.285	0.276	0.316	0.326	0.220
CCH_3SiH_3	aa	0.269	0.264	0.278	0.294	0.289	1.452	0.294	0.247	0.247	0.254	0.284	0.287	0.220
$C(SiH_3)_2$	aa	0.233	0.228	0.242	0.265	0.260	2.130	0.265	0.218	0.218	0.228	0.245	0.249	0.218
MUE for (a)		0.234	0.231	0.247	0.247	0.243	1.177	0.221	0.188	0.219	0.209	0.250	0.265	0.156
MUE for (a)–(b)		0.229	0.227	0.244	0.227	0.226	1.511	0.223	0.182	0.222	0.203	0.241	0.248	0.164
MUE for (a)–(d)		0.528	...	...	0.604	0.596	...	0.612	0.506	...	0.524	0.602	...	...
MUE for (a)–(g)		1.052	...	...	1.195	1.195	...	...	0.954	...	1.098	1.165	...	...

active space is indeed important, as discussed in Sec. II. Using ROHF/SR-CCSD(T) values as benchmarks, we find that ROHF/TD-CCSD significantly outperforms the ROHF/SR-CCSD method, indicating that effects normally attributable to triples in the SR framework are being folded in by the multi-reference framework of the TD-CCSD approach. Furthermore, it is worth mentioning that, just as the optimal orbitals for triplet states (ROHF) provide the best TD-CCSD triplet energies, the optimal orbitals for OSS states (TD-SCF) provide the best TD-CCSD OSS energetics.

For convenience, the remainder of this study will only compare the TD-CCSD results generated using the conventional RHF orbitals and the SA-MCSCF orbitals. The latter are chosen over ROHF or TD-SCF because they give an unbiased description of the two states of interest for obtaining $S_1 - T_0$ gaps within a single TD-CCSD calculation. To further explore trends in the TD-CCSD data used to compile Table I, Secs. IV B and IV C adopt a graphical approach for data analysis.

B. Comparison of TD-CC, EOMCC, and SR-CC triplet energies

In Sec. IV A, it was shown by comparison against ROHF/CCSD(T) energy benchmarks that TD-CCSD energies are dependent upon the reference orbitals. However, ROHF/CCSD(T) T_0 energies are a somewhat poor choice of benchmark due to the resulting large MUEs, often of the order of 1.0 eV. The similar magnitude of MUEs produced by the ROHF/SR-CCSD, RHF/TD-CCSD, and SA-MCSCF/TD-CCSD methods invites a more direct comparison of the three sets. In Fig. 2, the relative performance of RHF/TD-CCSD and SA-MCSCF/TD-CCSD is again considered, this time using both ROHF/SR-CCSD(T) and ROHF/SR-CCSD T_0 energies as benchmarks.

The correlation plot in Fig. 2(a) compares TD-CCSD errors produced using the RHF and SA-MCSCF reference orbitals, with ROHF/SR-CCSD(T) energies used as benchmarks. The resulting large MUEs and mean signed errors (MSEs) differ by only ∼10% and the best-fit line, which can be used as another metric for evaluating relative performance, has a strong coefficient of variation ($r^2 = 0.99$), a slope only slightly smaller than unity ($\frac{dy}{dx} = 0.95$), and an intercept of −0.02 eV. These results downplay the reference-dependence of the TD-CCSD energies.

Figure 2(b) differs from Fig. 2(a) in that the reference values are ROHF/SR-CCSD rather than ROHF/SR-CCSD(T). Here, due to the appropriate error magnitude, the superior performance of SA-MCSCF/TD-CCSD is immediately evident from the near-horizontal ($\frac{dy}{dx} = 0.01$) best-fit line with an intercept of 0.01 eV. Using the ROHF/SR-CCSD benchmarks, the TD-CCSD MSE is reduced by an order of magnitude switching from the RHF to SA-MCSCF reference orbitals, while the MUE is reduced by a factor of three. Each data subset is clustered closely about the zero of the ordinate, with the exception of the *m*-xylylenes, which were previously identified to have a significant multi-reference character.

Since the ROHF/SR-CCSD method cannot generate the OSS of interest in this work, comparisons need to be made with a method that can, hence, RHF/EOMCCSD. In the first instance, we examine its performance for producing T_0 total energies. Figure 3 plots the correlation between T_0 energy errors for RHF/EOMCCSD and TD-CCSD using RHF and SA-MCSCF reference orbitals. All values are again taken with respect to the ROHF/CCSD benchmark T_0 values, as was done in Fig. 2(b), to maintain small error magnitudes for easier interpretation.

The correlation plot in Fig. 3(a) compares TD-CCSD and EOMCCSD T_0 energy errors with the same RHF reference orbitals employed in both cases. The resulting MSEs and MUEs indicate that RHF/EOMCCSD outperforms RHF/TD-CCSD by 38% and 25%, respectively. The best-fit line is again almost horizontal with an intercept ∼0.1 eV, signifying a systematic overestimation by RHF/TD-CCSD, but this is not too meaningful given that the coefficient of determination is nearly zero ($r^2 = 0.01$).

In Fig. 3(b), the TD-CCSD reference orbitals are changed from RHF to SA-MCSCF(2,2). Remarkably, Fig. 3(b) completely reverses the trends of Fig. 3(a), showing SA-MCSCF/TD-CCSD significantly outperforming RHF/EOMCCSD. Comparing Figs. 3(a) and 3(b), it is clear that many inaccurate RHF/TD-CCSD T_0 energies are corrected by changing the reference orbitals, with most points in Fig. 3(b) being neatly clustered about the ordinate zero ($r^2 = 0.50$). The TD-CCSD MSE is an order of magnitude lower than that for RHF/EOMCCSD, while the MUE is also less by a factor of two. The small slope (0.39) and intercept (−0.02 eV) of the best-fit line provide supporting evidence of the excellent performance of SA-MCSCF/TD-CCSD.

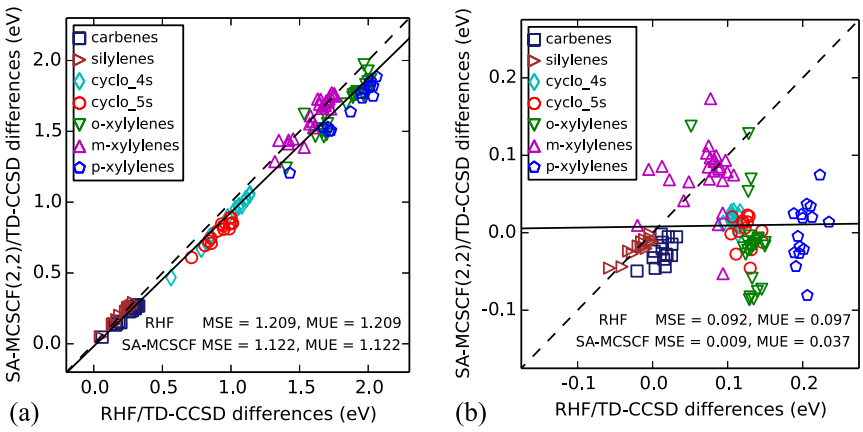

FIG. 2. Correlation between T_0 energy errors produced by TD-CCSD used with the RHF and SA-MCSCF reference orbitals. The least-squares fitted line of SA-MCSCF/TD-CCSD data is provided (solid) to be compared with the hypothetical perfectly correlated line (dashed), corresponding to the RHF/TD-CCSD values. Errors are taken with respect to ROHF/CCSD(T) values in (a) and ROHF/CCSD values in (b).

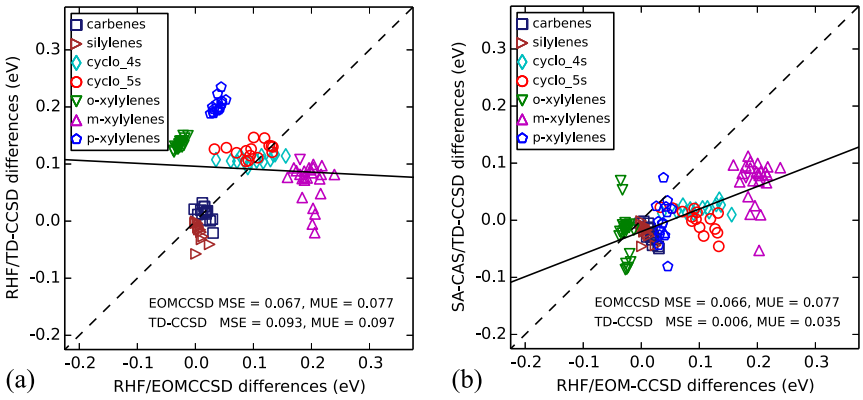

FIG. 3. Correlation between T_0 energy errors produced by RHF/EOMCCSD and TD-CCSD using (a) the RHF and (b) the SA-MCSCF reference orbitals. The least-squares fitted line of SA-MCSCF/TD-CCSD data is provided (solid) to be compared with the hypothetical perfectly correlated line (dashed), corresponding to the RHF/TD-CCSD values. Errors are reported with respect to ROHF/CCSD values.

In Fig. 3(b), the most extreme outliers are cycloalkanediyls and *m*-xylylenes. The poor performance of RHF/EOMCCSD for these species can be understood by examining the quality of the RHF/CCSD references used to construct the RHF/EOMCCSD states. For many of these systems, the magnitude of the underlying RHF/SR-CCSD t_2 amplitudes from the HOMO to LUMO determinant are 0.175 or more. This large static (non-dynamic) correlation effect in the S_0 state means that the RHF/SR-CCSD wavefunction might be poorly represented and, consequently, the resulting RHF/EOMCCSD state might not offer as good an approximation as normal. Though not strictly comparable because of the difference in the reference state, the amplitudes relative to the reference TD state are much smaller, with the *largest* RHF/TD-CCSD t_2 amplitude for a *m*-xylylene system being only 0.118 and the largest SA-MCSCF/TD-CCSD t_2 amplitude being only 0.079.

C. Comparison of TD-CC, EOMCC, and MREOM for open-shell singlet energies and $S_1 - T_0$ gaps

Open-shell singlet states make up the other half of the $S_1 - T_0$ splittings, and good benchmarks for such states must be generated using a reliable MR method, in this case MREOM. In this section, MREOM benchmark values are generated using the SA-MCSCF(2,2) reference orbitals. The expense of generating even the smallest (2,2) SA-MCSCF(2,2) reference orbitals limits our MREOM consideration to xylylene species with $X = Y = H$ (see Fig. 1). Some cyclo_4 and cyclo_5 species also had to be omitted due to convergence issues.

Correlation plots examining the orbital-dependence of TD-CCSD are again shown in Fig. 4, this time with MREOM providing the benchmark values. Here, TD-CCSD and SA-MCSCF(2,2)/MREOM S_1 energy differences are very large, hindering data analysis similar to the situation in Fig. 2(a). Although it is not shown, comparison of TD-CCSD and MREOM T_0 energies produces a quantitatively similar correlation plot to Fig. 4(a). This similarity of the correlation plots for T_0 and S_1 energy errors indicates that $S_1 - T_0$ gap errors may be much smaller and therefore more interpretable.

In Fig. 4(b), $S_1 - T_0$ gap errors are plotted, again comparing the TD-CCSD performance using the two reference orbital choices. As expected, errors are much smaller than those in Fig. 4(a), and, somewhat surprisingly, RHF/TD-CCSD outperforms SA-MCSCF(2,2)TD-CCSD, with the best-fit line having a slope of 1.46, an intercept of 0.06 eV, and a relatively tight scatter (r^2 = 0.80). The MSEs and MUEs for RHF/TD-CCSD are also ~50% better than those for SA-MCSCF(2,2)TD-CCSD.

The SA-MCSCF(2,2)/MREOM benchmarks are also useful for directly comparing the performance of TD-CCSD and EOMCCSD for generating $S_1 - T_0$ gaps, which are the subject of the correlation plots in Fig. 5. Figure 5(a) compares TD-CCSD and EOMCCSD with each employing RHF reference orbitals, while Fig. 5(b) compares SA-MCSCF/TD-CCSD and RHF/EOMCCSD. Both plots show TD-CCSD outperforming RHF/EOMCCSD, with the best-fit lines in Figs. 5(a) and 5(b) having slopes of 0.34 and 0.56 and intercepts of 0.02 and 0.10 eV, respectively. Considering instead the MSE and MUE values, RHF/TD-CCSD performs over twice as well as

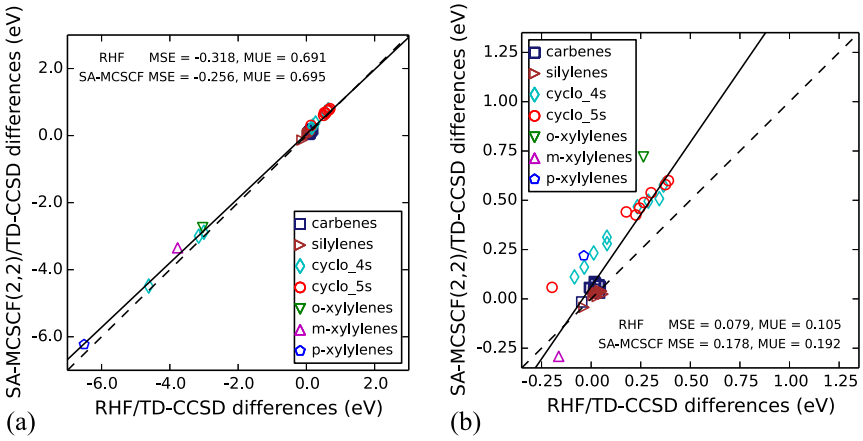

FIG. 4. Correlation between (a) open-shell singlet energy errors and (b) the singlet-triplet splitting errors, as produced by TD-CCSD using the RHF and SA-MCSCF reference orbitals. The least-squares fitted line of RHF/TD-CCSD data is provided (solid) to be compared with the hypothetical perfectly correlated line (dashed). All errors are reported with respect to SA-MCSCF(2,2)/MREOM values.

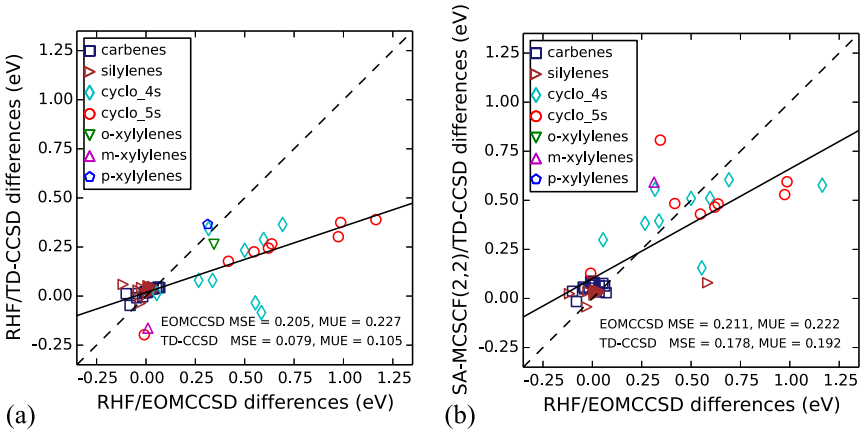

FIG. 5. Correlation between singlet-triplet splitting errors, as produced by RHF/TD-CCSD and RHF/EOMCCSD approaches. The least-squares fitted line of the TD-CCSD data is provided (solid) to be compared with the hypothetical perfectly correlated line (dashed). All errors are taken with respect to SA-MCSCF(2,2)/MREOM values.

RHF/EOMCCSD, while SA-MCSCF/TD-CCSD also beats out RHF/EOMCCSD by over 10%.

In Fig. 5, the cycloalkanediyls and xylylenes are again shown to be problematic for the RHF/EOMCCSD method. In Sec. IV B, similar discrepancies for T_0 energies were thought to originate from a poorly described RHF/SR-CCSD energy baseline. When the underlying RHF/SR-CCSD is a poor approximation, RHF/EOMCCSD triplet and OSS states will both be malformed and, since the resulting energy errors can be additive, $S_1 - T_0$ gap errors can grow as large as 1.0 eV, as shown in Fig. 5. For comparison, the $S_1 - T_0$ gaps generated by the reference MREOM method are themselves only 3.0–4.5 eV, so a 1.0 eV error is quite large. In Sec. IV D, additional EOMCC, TD-CC, and MREOM approaches are tested for their ability to generate $S_1 - T_0$ gaps.

D. Effect of enlarging the active space in TD-CCSD and MREOM calculations

One possible reason for the broad scatter in Figs. 4 and 5 is that a more definitive set of $S_1 - T_0$ benchmarks is needed. Improved accuracy is achievable for MREOM calculations by systematically increasing the active space specified in the calculations. To alleviate the steep computational costs associated with such calculations, structures with $X = Y = H$ were reoptimized within the appropriate point group and at the MBPT(2)/6-31G* level. This enables MREOM calculations using (2,2) to (8,8) active spaces.

Table II collects $S_1 - T_0$ gaps for the newly symmetrized structures. For CH_2 and SiH_2, energy differences between all methods considered differ by less than 0.02 eV, but for other systems more interesting trends emerge. Considering instead the two cycloalkanediyl systems, RHF/TD-CCSD produces significantly better $S_1 - T_0$ gaps as compared with RHF/EOMCC methods, and, as before, switching to the SA-MCSCF reference orbitals further refines the TD-CCSD results. The poor performance of RHF/EOMCCSD can again be explained by the large t_2 amplitudes in the underlying RHF/CCSD references. We thus recommend that when large t_2 amplitudes are found in the RHF/CCSD reference function, there is significant static correlation present that may be better handled by TD-CCSD or other MRCC methods.

Values for the three xylylene configurational isomers in Table II reinforce that these are particularly difficult cases requiring large active-space references. According to the MREOM calculations, *o*-xylylene is the only isomer requiring the largest (8,8) reference space, while the *m*- and *p*-xylylenes

TABLE II. Calculated $S_1 - T_0$ gaps for symmetrized structures reported as raw values (upper) and as differences relative to the highest level of theory considered (lower), in eV.

Method	Reference	CH_2	SiH_2	cyclo_4	cyclo_5	xyl_o	xyl_m	xyl_p
EOMCCSD	RHF	1.897	1.344	3.882	4.897	2.783	1.616	3.697
EOMCCSD(T)	RHF	1.895	1.324	3.865	4.897	2.792	1.454	3.729
TD-CCSD	RHF	1.885	1.347	3.657	4.287	2.702	1.427	3.749
	SA-MCSCF(2,2)	1.904	1.341	3.594	4.252	2.719	0.596	3.753
	SA-MCSCF(4,4)	...	...	...	...	2.475	1.129	3.820
MREOM	SA-MCSCF(2,2)	1.824	1.291	3.277	3.888	2.740	−0.020	3.791
	SA-MCSCF(6,6)	...	...	...	...	2.494	1.174	2.396
	SA-MCSCF(8,8)	...	...	...	...	2.295	1.163	2.306
EOMCCSD	RHF	0.073	0.053	0.605	1.009	0.488	0.453	1.391
EOMCCSD(T)	RHF	0.071	0.033	0.588	1.009	0.497	0.291	1.423
TD-CCSD	RHF	0.061	0.086	0.380	0.399	0.407	0.264	1.443
	SA-MCSCF(2,2)	0.080	0.050	0.317	0.364	0.424	−0.567	1.447
	SA-MCSCF(4,4)	...	...	...	...	0.180	−0.034	1.514
MREOM	SA-MCSCF(2,2)	...	...	...	...	0.445	−1.183	1.485
	SA-MCSCF(6,6)	...	...	...	...	0.199	0.011	0.090

require at least a (6,6) reference space to reach satisfactory agreement (<0.1 eV). Methods employing the RHF reference orbitals, including EOMCC and TD-CC methods, perform poorly, overestimating these $S_1 - T_0$ gaps by 15%–63%.

Further improvement of the TD-CCSD reference orbitals was also tested. Enlarging the active-space of the reference CSF from SA-MCSCF(2,2) to SA-MCSCF(4,4) improves the xylylene $S_1 - T_0$ gaps in almost all cases, with *m*-xylylene improving by 0.5 eV (46%). Only for the *p*-xylylene system does the energy worsen, but by a relatively small amount. This provides strong evidence that when the static correlation is properly described at the level of the reference orbitals, TD-CCSD provides an excellent treatment of the dynamical correlation required to accurately describe OSS excited states.

V. SUMMARY

A large set of biradical systems was considered to evaluate triplet and open-shell singlet total energies and $S_1 - T_0$ splittings produced by the TD-CCSD method. When using the conventional RHF reference orbitals, TD-CCSD triplet total energies were shown to be comparable in quality to those produced by ROHF/SR-CCSD. By performing TD-CCSD computations starting with several other sets of reference orbitals, it was found that absolute and relative TD-CC energies are influenced significantly by the reference orbitals chosen. Employing KS-DFT reference orbitals or the Brueckner doubles variant did not cause an overall improvement of the results. On the other hand, choosing ROHF, TD-SCF, or SA-MCSCF(2,2) CSFs as reference orbitals resulted in substantial improvements in the accuracy of TD-CCSD total energies.

The large test set of biradicals was used to make further comparisons between the performance of the RHF/TD-CCSD, SA-MCSCF(2,2)/TD-CCSD, and RHF/EOMCCSD approaches. For T_0 total energies, SA-MCSCF(2,2)/TD-CCSD outperformed RHF/EOMCCSD by a factor of two. A similar comparison between TD-CCSD and EOMCCSD was made for $S_1 - T_0$ gaps and the RHF/EOMCCSD method was again outperformed by a factor of two, this time by RHF/TD-CCSD. The relatively poor performance of RHF/EOMCCSD was traced back to underlying RHF/SR-CCSD ground-state wavefunctions having large t_1 and t_2 amplitudes. By contrast, TD-CCSD amplitudes remained small and thus provided a better approximation of the multi-reference nature of the states.

To definitively explain the large discrepancies produced by the SA-MCSCF/TD-CCSD and RHF/EOMCCSD approaches for the $S_1 - T_0$ splittings, refined MREOM values were generated using larger active spaces, up to and including (8,8). The TD-CCSD method is found to be successful in some cases where RHF/EOMCCSD fails, in particular when the underlying RHF/CCSD ground-state wavefunction is poorly described in the RHF/EOMCCSD calculation, as can happen when multi-reference character intrudes. For such cases, TD-CCSD $S_1 - T_0$ gaps can be more accurate, in some cases by over 1.0 eV, making TD-CCSD the strongly preferred alternative for describing $S_1 - T_0$ gaps involving biradical states. We demonstrate this for the exemplary cases of the cycloalkanediyl and xylylene systems.

The TD-CCSD method has been shown to be a promising alternative to RHF/EOMCCSD for the generation of certain excited states. In addition, the analysis of TD-CCSD amplitudes is straightforward, as the starting point is a spin-adapted configuration based on the particular occupied-virtual excitation. This leaves little ambiguity in the assignment of states during geometry optimizations or when facing near-degeneracies.

Future work will involve formulation and implementation of a perturbative extension to TD-CCSD accounting for connected triples excitations, i.e., TD-CCSD(T). This method is expected to provide a significant improvement over EOM-CCSD(T) for the description of triplet and open-shell singlet states, as well as $S_1 - T_0$ gaps. Further investigation of formal aspects of the SA-MCSCF/TD-CCSD method is also warranted, including consideration of its performance for describing single-bond-breaking potential energy curves and electric and magnetic properties.

SUPPLEMENTARY MATERIAL

See supplementary material for tables of geometries and individual TD-CCSD values used to generate the correlation plots in this work.

ACKNOWLEDGMENTS

This work was supported by funding from the U.S. DoD High Performance Computing Modernization Program and a grant of computer time at the U.S. Air Force Research Laboratory DoD Supercomputing Research Center. Additionally, J.J.L. was supported in part by an appointment to the Faculty Research Participation Program at the U.S. Air Force Institute of Technology (AFIT), Department of Engineering Physics, administered by the Oak Ridge Institute for Science and Education through an interagency agreement between the U.S. Department of Energy and AFIT. The views expressed in this work are those of the authors and do not reflect the official policy or position of the United States Air Force, Department of Defense, or the United States Government.

[1] R. J. Bartlett, Annu. Rev. Phys. Chem. **32**, 359 (1981).
[2] R. J. Bartlett and M. Musiał, Rev. Mod. Phys. **79**, 291 (2007).
[3] R. J. Bartlett, M. Musial, V. F. Lotrich, and T. Kus, in *Recent Progress in Coupled-Cluster Methods*, edited by P. Carsky, J. Paldus, and J. Pittner (Springer, Dordrecht, 2010), Chap. 1, Vol. 11, pp. 1–34.
[4] G. D. Purvis III and R. J. Bartlett, J. Chem. Phys. **76**, 1910 (1982).
[5] M. Urban, J. Noga, S. J. Cole, and R. J. Bartlett, J. Chem. Phys. **83**, 4041 (1985).
[6] K. Raghavachari, G. W. Trucks, J. A. Pople, and M. Head-Gordon, Chem. Phys. Lett. **157**, 479 (1989).
[7] J. D. Watts, J. Gauss, and R. J. Bartlett, J. Chem. Phys. **98**, 8718 (1993).
[8] V. Lotrich, N. Flocke, M. Ponton, A. Yau, A. Perera, E. Deumens, and R. Bartlett, J. Chem. Phys. **128**, 194104 (2008).
[9] J. Brabec, S. Krishnamoorthy, J. J. Hubertus, K. Kowalski, and J. Pittner, Chem. Phys. Lett. **514**, 347 (2011).
[10] N. Flocke and R. J. Bartlett, J. Chem. Phys. **121**, 10935 (2004).
[11] A. A. Auer and M. Nooijen, J. Chem. Phys. **125**, 024104 (2006).
[12] W. Li, P. Piecuch, J. R. Gour, and S. H. Li, J. Chem. Phys. **131**, 114109 (2009).
[13] J. J. Eriksen, P. Baudin, P. Ettenhuber, K. Kristensen, T. Kjærgaard, and P. Jørgensen, J. Chem. Theory Comput. **11**, 2984–2993 (2015).

[14]J. Pipek and P. G. Mezey, J. Chem. Phys. **90**, 4916 (1989).
[15]G. Knizia, J. Chem. Theory Comput. **9**, 4834 (2013).
[16]F. Aquilante, T. B. Pedersen, A. M. S. de Merás, and H. Koch, J. Chem. Phys. **125**, 174101 (2006).
[17]D. G. Liakos and F. Neese, J. Chem. Theory Comput. **11**, 4054 (2015).
[18]D. I. Lyakh, M. Musiał, V. F. Lotrich, and R. J. Bartlett, Chem. Rev. **112**, 182 (2012).
[19]J. F. Stanton and R. J. Bartlett, J. Chem. Phys. **98**, 7029 (1993).
[20]J. Geertsen, M. Rittby, and R. J. Bartlett, Chem. Phys. Lett. **164**, 57 (1989).
[21]D. C. Comeau and R. J. Bartlett, Chem. Phys. Lett. **207**, 414 (1993).
[22]M. Nooijen, Int. J. Mol. Sci. **3**, 656 (2002).
[23]H. Monkhorst, Int. J. Quantum Chem. **12**(S11), 421 (1977).
[24]E. Dalgaard and H. Monkhorst, Phys. Rev. A **28**, 1217 (1983).
[25]D. Mukherjee and P. Mukherjee, Chem. Phys. **39**, 325 (1979).
[26]M. Takahashi and J. Paldus, J. Chem. Phys. **85**, 1486 (1986).
[27]H. Koch and P. Jørgensen, J. Chem. Phys. **93**, 3333 (1990).
[28]H. Koch, H. J. A. Jensen, P. Jørgensen, and T. Helgaker, J. Chem. Phys. **93**, 3345 (1990).
[29]J. D. Watts and R. J. Bartlett, J. Chem. Phys. **101**, 3073 (1994).
[30]J. D. Watts and R. J. Bartlett, Chem. Phys. Lett. **233**, 81–87 (1995).
[31]J. D. Watts and R. J. Bartlett, Chem. Phys. Lett. **258**, 581–588 (1996).
[32]T. J. Watson, Jr., V. F. Lotrich, P. G. Szalay, A. Perera, and R. J. Bartlett, J. Phys. Chem. A **117**, 2569 (2013).
[33]S. Villaume, C. Daniel, A. Strich, S. A. Perera, and R. J. Bartlett, J. Chem. Phys. **122**, 044313 (2005).
[34]R. A. Chiles and C. E. Dykstra, J. Chem. Phys. **74**, 4544 (1981).
[35]L. Adamowicz, W. D. Laidig, and R. J. Bartlett, Int. J. Quantum Chem. **26**(S18), 245 (1984).
[36]M. Rittby and R. J. Bartlett, J. Chem. Phys. **92**, 3033 (1988).
[37]J. Gauss, W. J. Lauderdale, J. F. Stanton, J. D. Watts, and R. J. Bartlett, Chem. Phys. Lett. **182**, 207 (1991).
[38]G. D. Purvis, H. Sekino, and R. J. Bartlett, Collect. Czech. Chem. Commun. **53**, 2203 (1988).
[39]P. G. Szalay and J. Gauss, J. Chem. Phys. **112**, 4027 (2000).
[40]X. Li and J. Paldus, Phys. Chem. Chem. Phys. **11**, 5281 (2009).
[41]S. A. Kucharski and R. J. Bartlett, J. Chem. Phys. **95**, 8227 (1991).
[42]J. F. Stanton, J. Gauss, S. A. Perera, A. Yau, J. D. Watts, M. Nooijen, N. Oliphant, P. G. Szalay, W. J. Lauderdale, S. R. Gwaltney, S. Beck, A. Balková, D. E. Bernholdt, K.-K. Baeck, P. Rozyczko, H. Sekino, C. Huber, J. Pittner, and R. J. Bartlett, "ACESII is a product of the quantum theory project, University of Florida," integral packages included are VMOL (J. Almölf and P. R. Taylor), VPROPS (P. R. Taylor), and ABACUS (T. Helgaker, H. J. Aa. Jensen, P. Jørgensen, J. Olsen, and P. R. Taylor).
[43]A. Balková and R. J. Bartlett, J. Chem. Phys. **102**, 7116 (1995).
[44]A. Balková and R. J. Bartlett, J. Chem. Phys. **101**, 8972 (1994).
[45]A. Balková and R. J. Bartlett, J. Chem. Phys. **99**, 7907 (1993).
[46]A. Balková and R. J. Bartlett, Chem. Phys. Lett. **193**, 364 (1992).
[47]P. G. Szalay and R. J. Bartlett, J. Chem. Phys. **101**, 4936 (1994).
[48]J. F. Stanton, J. Gauss, M. E. Harding, P. G. Szalay, A. A. Auer, R. J. Bartlett, U. Benedikt, C. Berger, D. E. Bernholdt, Y. J. Bomble, O. Christiansen, M. Heckert, O. Heun, C. Huber, T.-C. Jagau, D. Jonsson, J. Jusélius, K. Klein, W. J. Lauderdale, D. A. Matthews, T. Metzroth, D. P. O'Neill, D. R. Price, E. Prochnow, K. Ruud, F. Schiffmann, S. Stopkowicz, J. Vázquez, F. Wang, and J. D. Watts, CFOUR, coupled-cluster techniques for computational chemistry, a quantum-chemical program package, http://www.cfour.de.
[49]P. Neogrády, P. G. Szalay, W. P. Kraemer, and M. Urban, Collect. Czech. Chem. Commun. **70**, 951 (2005).
[50]P. Piecuch and J. Paldus, Theor. Chim. Acta **83**, 69 (1992).
[51]P. Piecuch, R. Toboła, and J. Paldus, Chem. Phys. Lett. **210**, 243 (1993).
[52]P. Piecuch and J. Paldus, Phys. Rev. A **49**, 3479 (1994).
[53]X. Li, P. Piecuch, and J. Paldus, Chem. Phys. Lett. **224**, 267 (1994).
[54]P. Piecuch and J. Paldus, J. Chem. Phys. **101**, 5875 (1994).
[55]P. Piecuch, X. Li, and J. Paldus, Chem. Phys. Lett. **230**, 377 (1994).
[56]P. Piecuch and J. Paldus, J. Phys. Chem. **99**, 15354 (1995).
[57]J. T. Margraf, A. Perera, J. J. Lutz, and R. J. Bartlett, J. Chem. Phys. **147**, 184101 (2017).
[58]A. Perera, R. W. Molt, V. F. Lotrich, and R. J. Bartlett, Theor. Chem. Acc. **133**, 1514 (2014).
[59]Z. B. Liu, L. M. J. Huntington, and M. Nooijen, Mol. Phys. **113**, 2999 (2015).
[60]L. M. J. Huntington, O. Demel, and M. Nooijen, J. Chem. Theory Comput. **12**, 114 (2016).
[61]L. M. J. Huntington and M. Nooijen, J. Chem. Phys. **142**, 194111 (2015).
[62]I. Shavitt and R. J. Bartlett, *Many-Body Methods in Chemistry and Physics* (Cambridge, New York, 2009).
[63]B. Jeziorski and H. J. Monkhorst, Phys. Rev. A **24**, 1668 (1981).
[64]L. Meissner, S. A. Kucharski, and R. J. Bartlett, J. Chem. Phys. **91**, 6187 (1989).
[65]R. J. Bartlett, Int. J. Mol. Sci. **3**, 579 (2002).
[66]X. Li and J. Paldus, J. Chem. Phys. **119**, 5320–5333 (2003).
[67]X. Li and J. Paldus, J. Chem. Phys. **119**, 5346–5357 (2003).
[68]X. Li and J. Paldus, Int. J. Quantum Chem. **99**, 914–924 (2004).
[69]X. Li and J. Paldus, J. Chem. Phys. **120**, 5890–5902 (2004).
[70]J. Paldus, X. Li, and N. D. Petraco, J. Math. Chem. **35**, 215–251 (2004).
[71]X. Li and J. Paldus, Mol. Phys. **104**, 661–676 (2006).
[72]X. Li and J. Paldus, Mol. Phys. **104**, 2047–2062 (2006).
[73]X. Li and J. Paldus, J. Chem. Phys. **124**, 034112 (2006).
[74]X. Li and J. Paldus, J. Chem. Phys. **133**, 184106 (2010).
[75]D. M. Silver and R. J. Bartlett, Phys. Rev. A **13**, 1 (1976).
[76]E. Fermi and E. Amaldi, Mem. Acad. Ital. **6**, 117 (1934).
[77]S. Krebs, Comput. Phys. Commun. **116**, 137 (1999).
[78]S. Rothenberg and E. R. Davidson, J. Chem. Phys. **45**, 2560 (1966).
[79]R. Diffenderfer and D. Yarkony, J. Phys. Chem. **86**, 5098 (1982).
[80]T. H. Dunning, Jr., J. Chem. Phys. **53**, 2823 (1970).
[81]T. H. Dunning, Jr. and P. J. Hay, *Methods of Electronic Structure Theory* (Plenum Press, New York, 1977).
[82]N. J. Mayhall and M. Head-Gordon, J. Chem. Phys. **141**, 044112 (2014).
[83]N. Suaud, R. Ruamps, N. Guihery, and J. Malrieu, J. Chem. Theory Comput. **8**, 4127 (2012).
[84]J. P. Malrieu, R. Caballol, C. J. Calzado, C. de Graaf, and N. Guihéry, Chem. Rev. **114**, 429 (2014).